An efficient hole transporting polymer for quantum dot light-emitting diodes

Wenhai Wu, Zhao Chen, Yunfeng Zhan,* Bochen Liu, Weidong Song, Yue Guo, Ji Yan, Xiaolong Yang, Zhi Zhou and Wai-Yeung Wong**

Dr. Z. Chen, W. Wu, Dr. Y. Zhan, B. Liu, Dr. W. Song, Dr. Y. Guo, and J. Yan
School of Applied Physics and Materials
Wuyi University
22 Dongcheng Village, Jiangmen 529020, P.R. China
E-mail: chenzhao2006@163.com; zhanyf6@163.com
Prof. W.-Y. Wong
Department of Applied Biology and Chemical Technology and Research Institute for Smart Energy, The Hong Kong Polytechnic University (PolyU), Hong Hom, Hong Kong, P.R. China and PolyU Shenzhen Research Institute, Shenzhen, 518057, P.R. China.
E-mail: wai-yeung.wong@polyu.edu.hk
Dr. X. Yang
School of Chemistry, MOE Key Laboratory for Nonequilibrium Synthesis and Modulation of Condensed Matter, Xi'an Key Laboratory of Sustainable Energy Material Chemistry, Xi'an Jiaotong University, Xi'an 710049, P.R. China.
Prof. Z. Zhou
School of Chemistry and Materials Science, Hunan Agricultural University, Changsha 410128, P.R. China

Keywords: hole transporting polymers, stabilized HOMOs, high hole conductivities, high efficiencies, quantum dot light-emitting diodes

Ideal hole transporting polymers used in quantum dot (QD) light-emitting diodes (QLEDs) should possess the features such as high conductivities and stabilized HOMOs (the highest occupied molecular orbitals). Herein, an efficient polymer (named CNPr-TFB) is achieved by rationally adding a relatively weak electron-withdrawing group (2-cyanopropan-2-yl, CNPr) on a TFB like hole transporting polymer. CNPr-TFB exhibits a superior hole conductivity and much more stabilized HOMO in comparison with TFB. Therefore, much more holes are delivered into the QD emissive layers (EMLs) and a balanced recombination of electron and hole in the QLEDs is achieved. The external quantum efficiencies (EQEs) of the red, green, blue and white QLEDs made by CNPr-TFB as the hole transporting layer (HTL) are 20.7%, 16.6%, 11.3% and 15.0%, respectively, which are increased by 1.4−2.3 times in comparison with those of devices based on the commonly used TFB HTL. Meanwhile, the CNPr-TFB based QLEDs also exhibit longer operation lifetimes than those of devices using the TFB HTL. These

results confirm that CNPr-TFB with the features of high conductivity and stabilized HOMO could be an excellent HTL material for the QLED applications

1. Introduction

Colloidal quantum dots (QDs) have received a great interest due to their distinctive features involving high photoluminescence yields (PLQYs), tunable and size-dependent emission wavelengths, narrow full widths at half maximum (FWHM) and low-cost fabrication process, making the QD based light-emitting diodes (QLEDs) promising candidates for next-generation lighting and displays.[1−5] In the past two decades, some significant breakthroughs in improving the efficiencies of QLEDs have been achieved through engineering the materials and device architectures, leading to the external quantum efficiencies (EQEs) of QLEDs to be comparable with those of organic LEDs.[6−10] Nevertheless, the use of insulating organic ligands (such as oleic acid, OA) and zinc sulphide (ZnS) shell materials, which possess extremely deep valance bands (VBs), provides the QLEDs a long-standing hole transporting challenge at the interface between hole transporting layers (HTLs) and QD emissive layers (EMLs).[8,11−14] It results in unbalanced charge carriers inside the QD EMLs since zinc oxide nanoparticles (ZnO NPs) with high electron conductivities and suitable conduction bands (CBs) are used as the electron transporting layers (ETLs),[15,16] significantly increasing the exciton quenching inside QD EMLs through nonradiative channels and restricting the efficiencies of QLEDs.[17−19]

To balance the holes and electrons inside the QD EMLs, one feasible solution that favours the hole transport is by using the HTL polymers with stabilized HOMOs and high hole conductivities.[11,12,20−23] However, it is still a great challenge to achieve the hole transporting polymers which simultaneously satisfy these requirements.[11,12,22] It is well known that the HOMO of an organic semiconductor is the highest bonding orbital occupied by the last electron. In general, the stabilization of HOMO energy level is easily achieved by using electron-withdrawing moieties to decrease the densities of electrons delocalized on the conjugation rings

or electron-rich moieties in the organic semiconductor.[24,25] It is noted that these electrons will be restricted on the electron-withdrawing moieties and the hole conductivities of organic layer will be bound to decrease.[26] It seems that the stabilized HOMOs and high hole conductivities of hole transporting polymers are incompatible. For example, the electron-rich triphenylamine (TPA) and fluorene moieties afford TFB (poly (9,9-dioctylfluorene-*co*-*N*-(4-(*sec*-butyl)phenyl)diphenylamine)) a higher hole mobility (μ_h) of ~1.0×10^{-2} cm^2 V^{-1} S^{-1} but a destabilized HOMO of −5.3 eV.[27] It is found that the HOMO (−5.8 eV) of PVK (poly(9-vinylcarbazole)) is stabilized due to the use of carbazole moiety. However, in comparison with TFB, the poorer electron-donating ability of carbazole moiety and non-conjugation based polyethylene polymer chain significantly decrease the μ_h (~2.5×10^{-6} cm^2 V^{-1} S^{-1}).[21,28] To date, the generally used TFB, PVK and poly-TPD (poly(*N*,*N*′-bis(4-butylphenyl)-*N*,*N*′-bis(phenyl)benzidine), which exhibit relatively destabilized HOMOs or low hole conductivities, would not be the perfect hole transporting polymers for the QLED applications.[11,27,28] Meanwhile, the research works focusing on the hole transporting polymers used in the QLEDs are really rare. Therefore, the development of efficient hole transporting polymers for their potential QLED applications is urgently needed.

By reasonably adding electron-withdrawing groups (such as cyano (CN) groups) on the highly conductive TFB hole transporting polymer, herein, an unreported polymer poly (9,9-dioctylfluorene-*co*-*N*-(4-((2-cyanopropan-2-yl)phenyl)diphenylamine) (CNPr-TFB in **Figure 1**a) with high hole conductivity and stablized HOMO is investigated. In comparison with TFB, CNPr-TFB possesses a much more stabilized HOMO energy level and superior hole conductivity, resulting in a better alignment of energy level between the QDs and the HTL polymers so that a much more balanced distribution of charge carriers inside the QD EMLs is achieved.[29,30] The EQEs of red, green, blue (RGB) and white QLEDs made by CNPr-TFB are 20.7%, 16.6%, 11.3% and 15.0%, which are at least 1.4-fold higher than those of the devices by using TFB as the HTL. Meanwhile, CNPr-TFB affords these devices higher luminance

values, lower applied voltages at the brightness of 1 000−10 000 cd m^{-2} and longer operation lifetimes. From these results, it is found that CNPr-TFB would be an excellent HTL for the QLED applications.

2. Results and discussion

Since TFB has been generally used as the HTL polymer for the QLED applications,[31−33] the chemical modification on the TFB framework may be a rational and feasible approach to achieve the hole transporting polymers with stabilized HOMOs and high hole conductivities. Therefore, some electron-withdrawing cyano (CN) groups are introduced into the organic framework of TFB to achieve two unreported polymers (Figure 1a).[34,35] The 2-cyanopropan-2-yl (CNPr) group was chosen for its unique features, such as weak electron-withdrawing property and no active hydrogen (*α−H*) atoms. The former decreases the electrons on the polymer chain, resulting in a much more stabilized HOMO energy level. Meanwhile, the sp^3−C (carbon) atoms in CNPr groups are used to weaken the interactions between the CN groups and aromatic rings so as to avoid the electron densities on the conductive polymer chain from excessively being decreased. Therefore, CNPr-TFB may remain the hole conductivity as high as TFB does. By adding two methyl groups between benzyl and CN groups, it removes the active *α−H* atoms which act as active reaction sites and may result in undesired by-products. In addition, by directly attaching the CN groups on the TPA moieties, another polymer poly (9,9-dioctylfluorene-*co*-*N*-(4-cyanophenyl)diphenylamine) (CN-TFB) was also synthesized to study the influence of strong electron-withdrawing group on the HOMO/LUMO distribution and conductivity of polymer. These polymers were ordered from Luminescence Technology Corp. (Lumtec) and directly used without any further processing. CNPr-TFB shows a crystal-like morphology and its solution is transparent and colourless. Meanwhile, the solutions prepared by the amorphous TFB and CN-TFB solids show pale yellow and brown, respectively (Figure 1b). Besides, the characteristic data for nuclear magnetic resonance (NMR) spectroscopy,

weight average molecular weight (M_w), Fourier transform infrared (FT-IR) spectroscopy (Figure S1) and thermogravimetric analysis (TGA) (Figure S2) are shown in Supporting Information (SI).

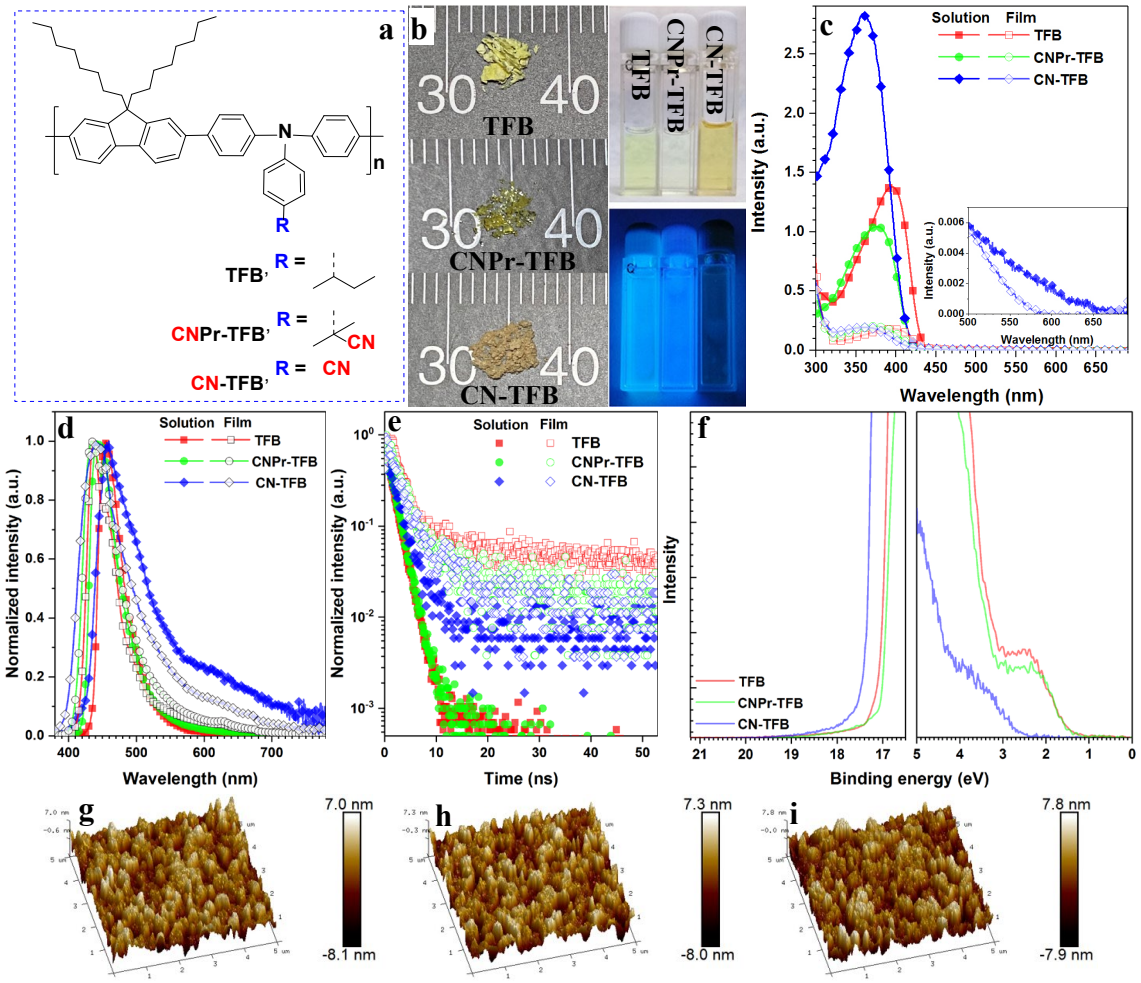

Figure 1. a) The chemical structures of TFB, CNPr-TFB and CN-TFB; b) the pictures of polymer solids and solutions under sunlight and UV radiation; c) the UV-visible absorption and d) photoluminescence spectra of the polymers; e) the photoluminescence decay curves of the polymer solutions and films; f) ultraviolet photoelectron spectrometer (UPS) spectra of polymer films; g)–i) atomic force microscopy (AFM) images for TFB, CNPr-TFB and CN-TFB films.

The polymer solutions (2 mg mL^{-1} in chlorobenzene) and thin films demonstrate a strong absorption at the wavelength of around 300–400 nm (Figure 1c), which is assigned to the π–π* transition arising from the fluorene and TPA moieties.[36,37] The absorption wavelength of over

500 nm is only observed in the spectra of CN-TFB due to the intramolecular charge-transfer (ICT) from the electron-donating conjugation rings to the CN groups (Figure 1c, inset).[38] The PL spectra of these polymers are shown in Figure 1d. The peak emission wavelengths are found at 453, 441 and 459 nm in the PL spectra of TFB, CNPr-TFB and CN-TFB solutions. Their films exhibit blue-shifted emissions and the emission wavelengths of 436, 433 and 441 nm for TFB, CNPr-TFB and CN-TFB are observed (Figure 1d and Table S1). It is found that the emission spectra measured in the TFB and CNPr-TFB solutions are structureless and mainly attributed to their fluorescent emissions (singlet excited states, S_1).[39] Meanwhile, due to the strong intermolecular interactions in the polymer films, some emission shoulders at the wavelength of around 450−500 nm are observed, which may be originated from the aggregated complexes, such as π excimers.[40] It is noted that the emission spectra of CN-TFB exhibit a broader emission region from 380 to 780 nm with another strong emission shoulder at the wavelength of around 620 nm. According to the result found in the absorption spectrum of CN-TFB, this shoulder is due to the ICT transitions which are usually characterized by the broad and low-energy emission features.[39,41,42] Moreover, the PLQYs of TFB, CNPr-TFB and CN-TFB films are 5.1% and 7.5% and < 0.1% (Table S1). It is found that the PLQY of CN-TFB is significantly smaller than those of TFB and CNPr-TFB, demonstrating a much stronger non-radiative process mainly originated from the defects or ICT transitions in the CN-TFB film.[38,39,41] The PL decay curves in Figure 1e are biexponential and tertiary exponential. In polymer solutions, the τ_1 (decay time constant) values of TFB, CNPr-TFB and CN-TFB are 1.42, 1.49 and 0.27 ns with the A_1 (amplitude) values of 97.29%, 97.89% and 6.4%, respectively. The τ_2 values of TFB, CNPr-TFB and CN-TFB are 7.86, 7.13 and 2.30 ns with the A_2 values of 2.71%, 2.11% and 93.60%, respectively (Table S1). The biexponential decay dynamics of these polymer solutions may be due to the excited states containing the dominant S_1 and aggregated complexes/ICT transitions.[40] In polymer films, the τ_1 (1.96 and 2.40 ns for TFB and CNPr-TFB) and τ_2 (15.70 and 14.51 ns for TFB and CNPr-TFB) values are lengthened and a

significant increase of A_2 (30.07% and 26.29% for TFB and CNPr-TFB) is observed due to the increased aggregation. In contrast to TFB and CNPr-TFB, the tertiary exponential decay is observed in the CN-TFB film, which may result from more than two kinetic processes such as the S_1 excited states, aggregated complexes and ICT transitions.[40,43] Besides, these decay curves for polymer/QD films reveal that the excitons formed inside the QD EMLs would be less quenched by the bottom CNPr-TFB HTL (Figure S4 and Table S2), corresponding to less defects in the CNPr-TFB film.[29]

Moreover, all the polymer films possess an indistinguishable surface morphology with the root-mean-square (RMS) roughness of around 2 nm, which are smooth enough to fabricate the QD films on the surfaces of polymer films (Figure 1g−1i). Most importantly, the ionization potential (IP) values (below vacuum level) of TFB, CNPr-TFB and CN-TFB films measured by the UPS are around 5.32, 5.50 and 6.02 eV (Figure 1f), corresponding to the HOMOs of −5.32, −5.50 and −6.02 eV, respectively (Table S1).[44] It is noted that the use of CN on the TPA moieties could stabilize the HOMOs of CNPr-TFB and CN-TFB.

To reveal how the CN groups affect the energy levels of polymers, the density functional theory (DFT) was used to calculate the HOMO and LUMO distributions of polymers.[45] Two fluorene-TPA units and propyl groups on the fluorene moieties were used to simplify the DFT calculations.[37] On the one hand, the HOMOs of TFB, CNPr-TFB and CN-TFB segments are mainly distributed on the electron-rich TPA and fluorene moieties (**Figure 2**). For example, the percentages of 56.97% for the HOMO contribution on TPA are found in CNPr-TFB, higher than those in TFB (52.82%) and CN-TFB (52.59%). Meanwhile, these HOMO contribution values on the fluorene moieties are less than 20%, significantly smaller than those observed on the TPA moieties. Therefore, chemical modification on the TPA moieties can tune the HOMO distributions of polymers. The CNPr and CN groups also own a slight HOMO distribution of 0.54% and 1.68%, respectively, but no HOMO contribution from the *sec*-butyl group. The calculated HOMOs of two organic units in TFB, CNPr-TFB and CN-TFB are −5.14, −5.33 and

−5.63 eV, respectively (Table S1), which agrees with the UPS results and shows the consistent tendency that electron-withdrawing groups on the TPA moieties can stabilize the HOMOs of polymers through pulling the electrons on the polymer chain to these electron-withdawing groups.[35] On the other hand, the LUMO energy levels are also distributed on the fluorene and TPA moieties in these polymers. In contrast to the HOMO contributions, TPA moieties have less LUMO contributions with the percentages of 22.89%, 22.83% and 25.68% for TFB, CNPr-TFB and CN-TFB, respectively. On the contrary, fluorene moieties own large LUMO contributions (55.43%, 54.50% and 51.75% for TFB, CNPr-TFB and CN-TFB). It is noted that the calculated LUMOs for TFB, CNPr-TFB and CN-TFB are −1.40, −1.53 and −1.77 eV, respectively (Table S1). From these results, it is found that the CNPr and CN groups on the TPA moieties can be used to stabilize the HOMOs of polymers. Much more stabilized HOMO of CN-TFB can be achieved due to the stronger interactions between CN and TPA moieties.

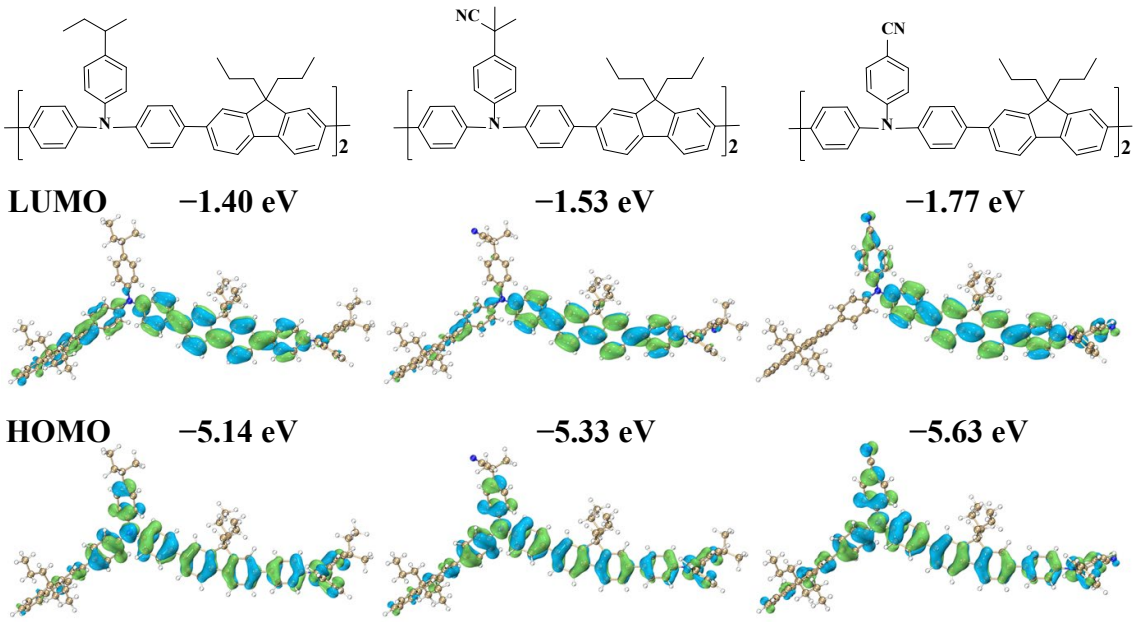

Figure 2. The calculated HOMO and LUMO energy levels of TFB, CNPr-TFB, CN-TFB.

However, the stabilized HOMOs cannot ensure the high hole conductivities of polymers. To investigate the conductive properties of these hole transporting polymers, the hole-only devices (HODs) with the architectures of ITO/PEDOT:PSS (poly(3,4-

ethylenedioxythiophene):poly(styrenesulfonate))/polymers/MoO_3 (molybdenum oxide)/aluminum (Al) were fabricated and characterized.[23] The current density (measured under a dark environment) of HOD made by CNPr-TFB is higher than those of the devices based on TFB and CN-TFB (**Figure 3**a), corresponding to an excellent hole conductivity of CNPr-TFB. On the one hand, the CN groups in CN-TFB are directly attached to the conjugated rings so as to pull much more electron densities to the CN groups, resulting in much more stabilized HOMO energy level. However, these electrons will be further restricted on these strong electron-withdrawing groups and difficult to freely move, leading to decreased hole conductivity of CN-TFB. Fortunately, the sp^3−C atoms between the CN groups and aromatic rings in CNPr-TFB can keep most of the electrons on the conductive polymer chain from being redistributed on these CN groups. Therefore, the chemical structure variation in CNPr-TFB not only stabilizes its HOMO energy level but also has less influence on its hole conductivity. On the other hand, the use of CNPr group assigns much more HOMO contributions to the TPA moieties in CNPr-TFB (HOMO contributions of 56.97%, 52.82% and 52.59% from the TPA moieties in CNPr-TFB, TFB and CN-TFB, respectively), being in favor of hole transport. Meanwhile, the HODs based on ITO/PEDOT:PSS/polymers/RGB QDs/MoO_3/Al and the electron-only devices (EODs) of ITO/ZnMgO (magnesium doped ZnO)/RGB QDs/ZnMgO/Al were also fabricated to further confirm the hole conductivity of CNPr-TFB in the presence of QD EMLs.[8] Due to the high hole conductivity and stabilized HOMO energy level, it is reasonable that the current densities of HODs based on CNPr-TFB/RGB QDs are higher than those of HODs made by other polymers and close to those of QDs based EODs (Figure S6). It confirms that the hole conductive capability of CNPr-TFB is significantly superior to those of TFB and CN-TFB, delivering much more holes into the QDs and achieving much balanced holes and electrons in the QD EMLs. In addition, the current densities of EODs (ITO/ZnMgO/polymers/ZnMgO/Al) based on TFB and CNPr-TFB are smaller by 0.3 mA cm^{-2}

at 4.5 V (Figure 3b), corresponding to the excellent electron blocking features of TFB and CNPr-TFB.

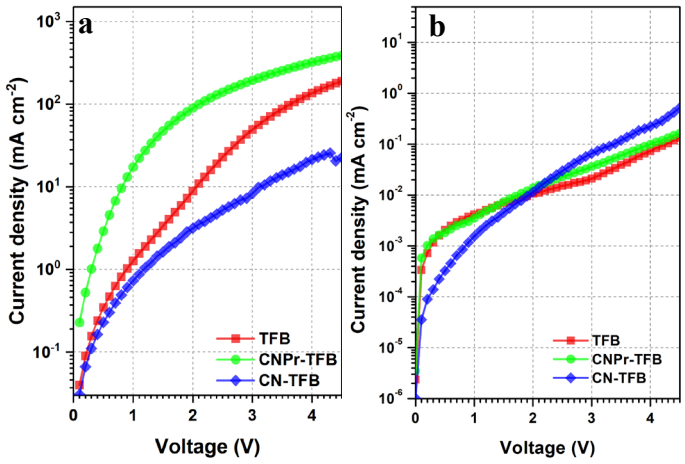

Figure 3. The *J*−*V* curves of single charge carrier devices: a) hole-only and b) electron-only devices based on the polymers.

By considering the features of high hole conductivity, stabilized HOMO, good electron blocking property and less defects, CNPr-TFB has a great potential as an excellent hole transporting polymer for QLED applications. The QLEDs were fabricated according to the device architecture of ITO/PEDOT:PSS (35 nm)/HTL polymers (30 nm)/RGB QDs (20 nm)/ZnMgO (50 nm)/Al (100 nm) (**Figure 4**a), where ITO and Al served as the electrodes, PEDOT:PSS as the hole injection layer (HIL), the polymer TFB or CNPr-TFB as the HTL, and ZnMgO as the ETL. The photophysics and VB characteristics of these commercial RGB QDs were studied. The QDs afford the peak emission wavelengths of 627, 528 and 463 nm with the PLQYs of 75.7%, 82.0% and 70.5% for RGB QDs, respectively. More details for the QDs will be found in SI (Figure S3−S5 and Table S2) without further discussion here. According to the UPS results (Figure S5 and Table S2), the energy diagrams of QLEDs in Figure 4b reveal that the energy barriers from the HOMO of CNPr-TFB to VBs of QDs are decreased, which can favour the hole injection and transportation into the QD EMLs. The electroluminescence (EL) spectra of the devices made by TFB and CNPr-TFB are indistinguishable for each colour and

the emission colours from these working devices are pure with the Commission Internationale de l'Eclairage (CIE) coordinates of (x = 0.69, y = 0.31), (x = 0.18, y = 0.77) and (x = 0.13, y = 0.07) for RGB QLEDs, respectively (Figure 4c, 4d and Table S3). In conjunction with the PL spectra measured from the QD films (Figure S3c), the emissions are assigned to the QDs rather than other functional layers. Due to the much more stabilized HOMO energy level and high hole conductivity in comparison with TFB, the electrons and holes inside the EMLs of the QLEDs based on CNPr-TFB may be much more balanced than the devices fabricated by TFB (Figure 3a and S6), resulting in higher EQEs and lower applied voltages at the luminance of 1 000−10 000 cd cm^{-2} (Figure 4e and 4f). The RGB QLEDs made by CNPr-TFB afford the EQEs of 20.7%, 16.6% and 11.3%, respectively, which are >1.4 times higher than those of the devices based on TFB (Figure 4e and Table S3). Although the use of CNPr-TFB decreases the energy barrier for hole transport from polymer to QDs, the electron transport in red and green QLEDs is still dominant (Figure S6a and S6b). On the other hand, the shallow CB of blue QD affords its QLED with a decreased electron transport, resulting in the much more balanced charge carriers inside the blue QLED made by CNPr-TFB (Figure S6c). Therefore, it is reasonable that the blue QLED based on CNPr-TFB exhibits a much more significant EQE increase than the red and green QLEDs. From these EQE curves, the blue QLED made by CNPr-TFB exhibits a relatively strong EQE roll-off in comparison with the red and green QLEDs. Except for the influence of the charge carriers inside the EMLs, the lower PLQY of blue QDs and much more defects on the surface of blue QDs arose from their small nanocrystal size also afford the blue QLEDs with a significantly EQE roll-off. It is noted that CNPr-TFB owns a stronger electron conductivity than TFB (Figure 3b), resulting in an electron leakage from blue QDs to CNPr-TFB at high applied voltages. Therefore, the EQE roll-off for the blue QLED made by CNPr-TFB is stronger than the device based on TFB. Meanwhile, the stabilized HOMO of CNPr-TFB results in low voltages of 3.9, 3.7 and 3.6 V at the luminance of 10 000 cd cm^{-2} for red and green QLEDs, 1 000 cd cm^{-2} for blue QLED, which are lower than those values found in TFB

based QLEDs (Figure 4e). Other hole-conductive polymers (such as CN-TFB, poly-TPD, PVK and TFB from different suppliers) were also used as the HTLs to fabricate the QLEDs. Unfortunately, these devices exhibit an inferior performance (such as low EQEs and high applied voltages at the luminance of 1 000−10 000 cd cm^{-2}) in comparison with those of QLEDs made by CNPr-TFB (Figure S8−S10 and Table S3). Last but not least, these devices made by CNPr-TFB exhibit longer operation lifetimes. For example, the lifetimes (T_{50}) at the half values of their initial luminance values for RGB QLEDs are 427, 360 and 15.8 hours, respectively (Figure S11), which are significantly higher than those of TFB based QLEDs (T_{50} = 135, 77 and 0.84 hours for RGB QLEDs). By considering the improved EQEs and stabilities, we believe that CNPr-TFB could be a better hole transporting polymer for QLED applications.

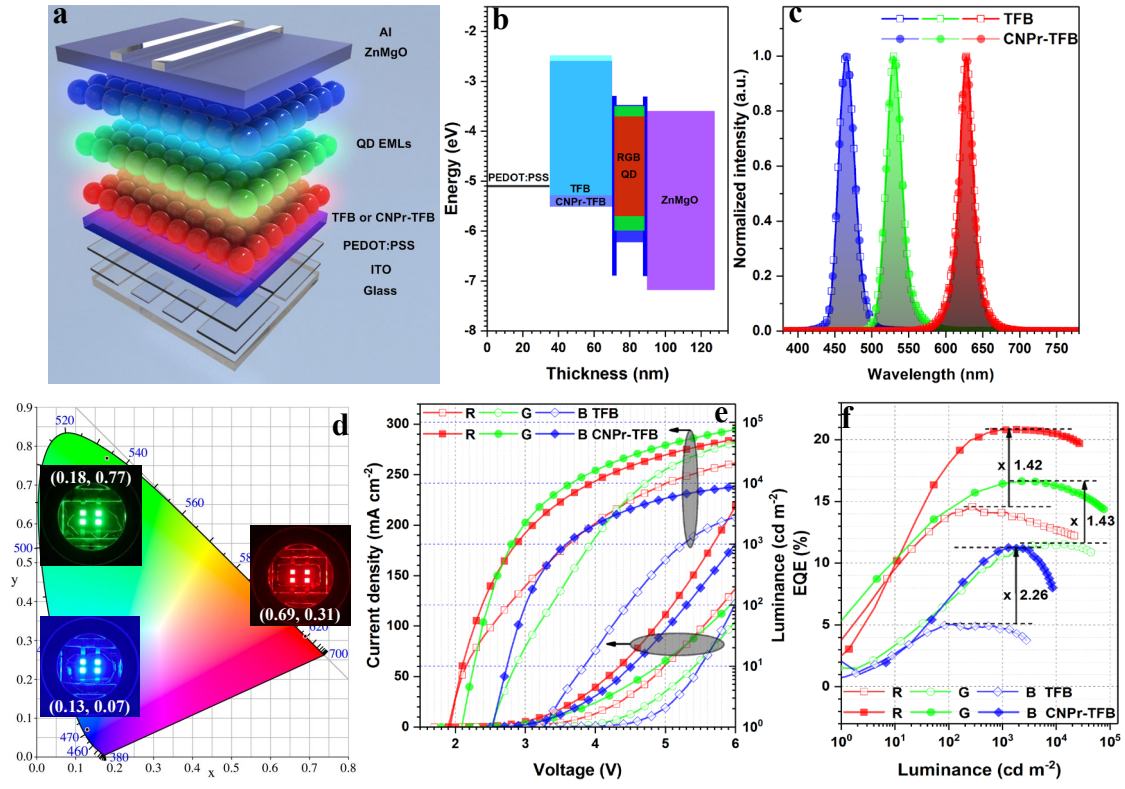

Figure 4. The performance of RGB QLEDs by using TFB and CNPr-TFB: a) and b) device structures and energy diagram of QLEDs; c) EL spectra; d) CIE coordinates and images of RGB QLEDs; e) *J*−*V*−*L* curves; f) EQE−*L* curves.

Since CNPr-TFB has a great potential to be one of the excellent hole-transporting polymers, its further application in the white QLEDs (WQLEDs) was also investigated. The WQLEDs were fabricated according to the device architecture of ITO/PEDOT:PSS (35 nm)/HTL polymers (30 nm)/RGB QDs (R:G:B = 1:4:10 by weight, 20 nm)/ZnMgO (50 nm)/Al (100 nm). As shown in **Figure 5**a and 5b, the light from red QD is firstly observed at lower applied voltages due to its lower energy gap. The emission intensities of blue and green QLEDs are gradually increased with the driving voltage and they are relatively stable when the luminance is higher than 1 000 cd m^{-2}. Therefore, the CIE coordinates of these two WQLEDs are shifted from the red to the nearby white region (Figure 5c and Table S4), which is commonly observed in other reported results.[46–49] Due to the highly efficient blue and green emissions, the CIE coordinates of the CNPr-TFB based WQLED (x = 0.37, y = 0.30) are close to the pure white (x = 0.33, y = 0.33) and they are kept at around (x = 0.37, y = 0.30) when the applied voltage is increased from 4 V to 6 V (Figure 5b−5d). Therefore, the variation values of CIE coordinates (Δx = 0.02, Δy = 0.01) are insignificant in the luminance region from 5 000 to 32 000 cd m^{-2}, corresponding to a relatively stable white emission (Figure 5b, 5c, S12b and Table S4). Meanwhile, it is noted that CNPr-TFB affords its WQLED with the luminance of over 32 000 cd m^{-2} at 6 V, which is higher than that of the device based on TFB (L < 15 000 cd m^{-2} at 6 V) (Figure 5e). Most importantly, the peak EQE of 15.0% (corresponding CIE coordinates of (x = 0.44, y = 0.32) and luminance of 340 cd m^{-2}) is found in the CNPr-TFB based WQLED, 1.90 times higher than that of the TFB based device (EQE = 7.8%, CIE coordinates of (x = 0.52, y = 0.37) and luminance of 420 cd m^{-2}) (Table S5). Although the CNPr-TFB based WQLED exhibits a significant EQE roll-off, the EQE of 10.5% is still attained at the luminance of around 10 000 cd m^{-2} with the CIE coordinates of (x = 0.37, y = 0.30) (Table S5), which is 1.8 times higher than that of device based on TFB and among the best WQLEDs fabricated by using mixed RGB QDs.[46–49] The significant EQE roll-off of the WQLED based on CNPr-TFB is mainly due to the poor performance of blue QLED at high applied voltages as discussed above,

which is also found in other literature reports.[46,50] Therefore, From these results, it is noted that the hole-transporting polymer CNPr-TFB is superior to the commonly used TFB HTL in the WQLED applications.

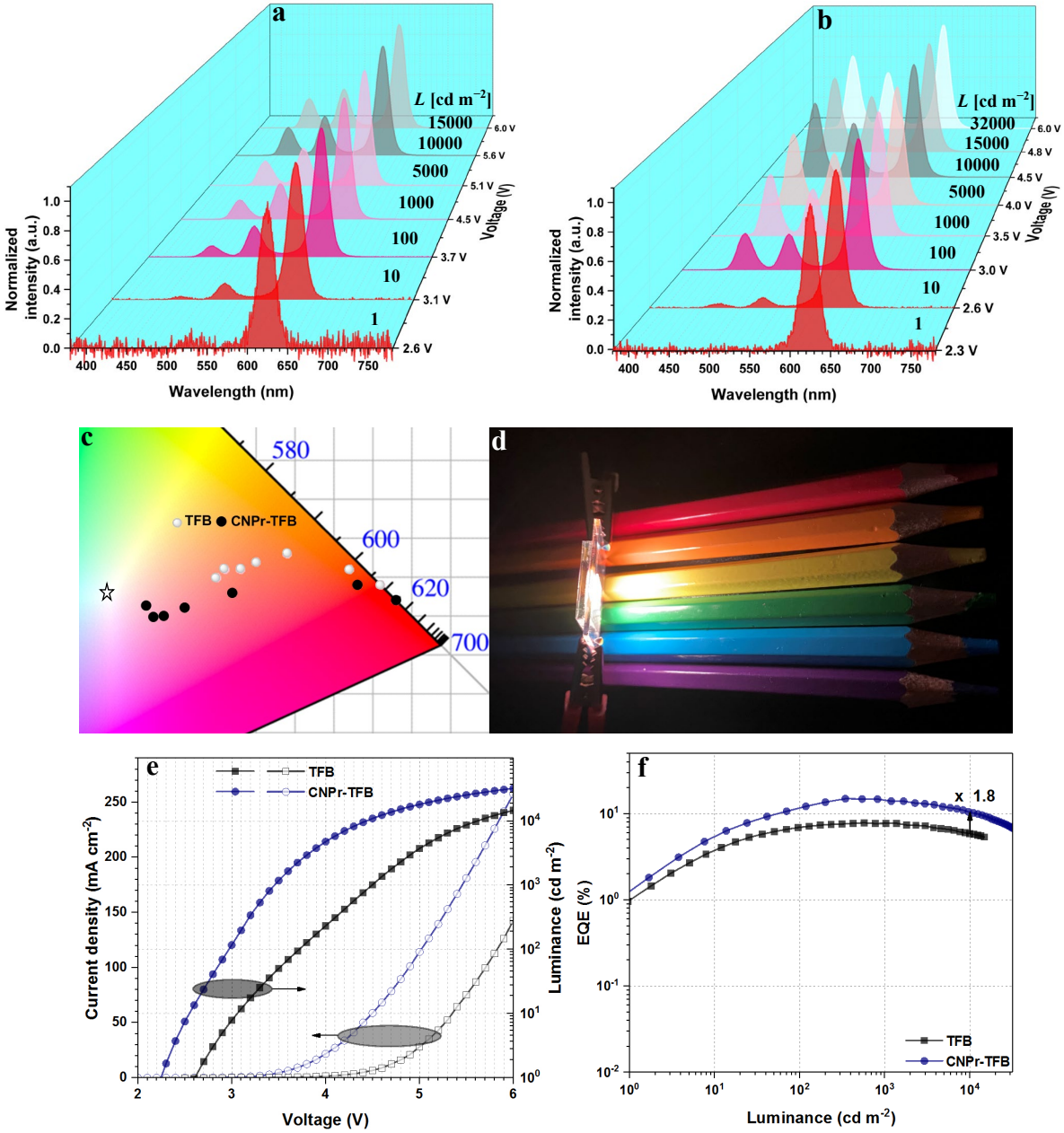

Figure 5. a) and b) EL spectra of WQLEDs made by TFB and CNPr-TFB, respectively; c) CIE coordinates; d) the image of working WQLED based on CNPr-TFB; e) and f) *J*–*V*–*L* and EQE–*L* curves of WQLEDs.

3. Conclusion

In conclusion, an unreported hole transporting polymer CNPr-TFB with stabilized HOMO and high hole conductivity was used to fabricate RGB and white QLEDs. CNPr-TFB affords its RGB and white light-emitting devices with higher EQEs (20.7%, 16.6%, 11.3% and 15.0% for RGB and white QLEDs) and luminance values, significantly superior to those devices made by the generally used TFB, PVK and Poly-TPD. It is mainly due to the fact that the weak electron-withdrawing group 2-cyanopropan-2-yl not only redistributes the HOMO contribution to stabilize the HOMO energy level so that the hole transporting barrier at the interface of HTL/EML is decreased, but also keeps the electrons on the conductive polymer chains from being restricted so as to retain its high hole conductivity. As a result, it transports much more holes inside the QD EMLs to achieve a balanced recombination of electron and hole and hence an excellent performance of its QLEDs. Meanwhile, CNPr-TFB quenches less excitons inside the QD EMLs, corresponding to less defects found inside the CNPr-TFB HTL. In addition, CNPr-TFB could be used as an electron blocking layer to efficiently confine the electrons inside the QD EMLs, affording its QLEDs a better performance. By considering the superior device performance, it is reasonable that CNPr-TFB with the features of stabilized HOMO, high hole conductivity, less defects and electron confinement could be used as one of the most efficient HTL for QLED applications.

4. Experimental Section

Device fabrication and measurements: The ITO substrates were pre-cleaned in ultrasonic cleaner with detergent and deionized water. After placing the ITO substrates under UV-O_3 for 30 minutes, PEDOT:PSS (HIL, ~35 nm) was fabricated on the surface of ITO substrates and annealed at 150 °C for 15 min in air. These substrates were then transferred into a nitrogen filled glove box. The hole transporting polymers (8−10 mg mL^{-1} in chlorobenzene) were spin-coated on the surface of PEDOT:PSS and annealed at 120 °C for 10 min to form ~30 nm HTLs.

The films of QD EMLs (~20 nm) were fabricated by spin-coating the RGB QDs (10 mg mL^{-1} in octane) on the HTLs and annealed at 90 °C for 5 min. Then, ZnMgO (20 mg mL^{-1} in ethanol) was spin-coated as the ETL (~ 50 nm). Lastly, the Al anode (100 nm) was thermally deposited under a pressure of 2×10^{-6} torr. The active area of the devices was 2 mm × 2 mm. The devices were encapsulated before measurement. The current−voltage (*I*−*V*) curves were measured by a dual-channel Keithley 2400 source meter. An external quantum efficiency measurement system (C9920−12, Hamamatsu Photonics, Japan) with an integrating sphere and multi-channel analyzer PMA−12 were used to collect the EL spectra, luminance values and EQEs.[51]

Supporting Information
Supporting Information is available from the Wiley Online Library or from the author.

Acknowledgements
This work was supported by the Key-Area Research and Development Program of Guangdong Province (No. 2020B010174004), the National Natural Science Foundation of China (No. 21901190), the Featured Innovation Projects of Colleges and Universities in Guangdong Province (Natural Science, No. 2018KTSCX232), the Guangdong Basic and Applied Basic Research Foundation (No. 2019A1515111201, 2019A1515110778) and Key Laboratory of Optoelectronic materials and Applications in Guangdong Higher Education (No: 2017KSYS011), the Science, Technology and Innovation committee of Shenzhen Municipality (JCYJ20180507183413211), the Hong Kong Research Grants Council (PolyU 123384/16P), Guangdong-Hong Kong-Macao Joint Laboratory of Optoelectronic and Magnetic Functional Materials (2019B121205002), the National Natural Science Foundation of China (No. 52073242), the Hong Kong Polytechnic University (1-ZE1C), Research Institute for Smart Energy (RISE) and Ms. Clarea Au for the Endowed Professorship in Energy (847S).

Received: ((will be filled in by the editorial staff))
Revised: ((will be filled in by the editorial staff))
Published online: ((will be filled in by the editorial staff))

References

[1] H. Moon, C. Lee, W. Lee, J. Kim, H. Chae, *Adv. Mater.*, **2019**, *31*, 1804294.

[2] Z. Yang, M. Gao, W. Wu, X. Yang, X. W. Sun, J. Zhang, H.-C. Wang, R.-S. Liu, C.-Y. Han, H. Yang, W. Li, *Mater. Today*, **2019**, *24*, 69.

[3] X. Dai, Y. Deng, X. Peng, Y. Jin, *Adv. Mater.*, **2017**, *29*, 1607022.

[4] H. Cho, J.-A. Pan, H. Wu, X. Lan, I. Coropceanu, Y. Wang, W. Cho, E. A. Hill, J. S. Anderson, D. V. Talapin, *Adv. Mater.*, **2020**, *32*, 2003805.

[5] E. Nannen, J. Frohleiks, S. Gellner, *Adv. Funct. Mater.*, **2020**, *30*, 1907349.

[6] J. Song, O. Wang, H. Shen, Q. Lin, Z. Li, L. Wang, X. Zhang, L. S. Li, *Adv. Funct. Mater.*, **2019**, *29*, 1808377.

[7] X. Dai, Z. Zhang, Y. Jin, Y. Niu, H. Cao, X. Liang, L. Chen, J. Wang, X. Peng, *Nature*, **2014**, *515*, 96.

[8] H. Shen, Q. Gao, Y. Zhang, Y. Lin, Q. Lin, Z. Li, L. Chen, Z. Zeng, X. Li, Y. Jia, S. Wang, Z. Du, L. S. Li, Z. Zhang, *Nat. Photonics*, **2019**, *13*, 192.

[9] H. Zhang, S. Chen, X. Sun, *ACS Nano*, **2018**, *12*, 697.

[10] H. Zhang, X. Sun, S. Chen, *Adv. Funct. Mater.*, **2017**, *27*, 1700610.

[11] H. Jia, F. Wang, Z. Tan, *Nanoscale*, **2020**, *12*, 13186.

[12] H. Qi, S. Wang, X. Jiang, Y. Fang, A. Wang, H. Shen, Z. Du, *J. Mater. Chem. C.*, **2020**, *8*, 10160.

[13] H. Shen, W. Cao, N. T. Shewmon, C. Yang, L. S. Li, J. Xue, *Nano Lett.*, **2015**, *15*, 1211.

[14] P. Reiss, M. Protière, L. Li, *Small*, **2009**, *5*, 154.

[15] Y. Sun, W. Wang, H. Zhang, Q. Su, J. Wei, P. Liu, S. Chen, S. Zhang, *ACS Appl. Mater. Interfaces*, **2018**, *10*, 18902.

[16] L. Qian, Y. Zheng, J. Xue, P. H. Holloway, *Nat. Photonics*, **2011**, *5*, 543.

[17] Q. Khan, A. Subramanian, I. Ahmed, M. Khan, A. Nathan, G. Wang, L. Wei, J. Chen, Y. Zhang, Q. Bao, *Adv. Optical Mater.*, **2019**, *7*, 1900695.

[18] M. C. Löbl, C. Spinnler, A. Javadi, L. Zhai, G. N. Nguyen, J. Ritzmann, L. Midolo, P. Lodahl, A. D. Wieck, A. Ludwig, R. J. Warburton, *Nat. Nanotechnol.*, **2020**, *15*, 558.

[19] J. P. Philbin, E. Rabani, *J. Phys. Chem. Lett.*, **2020**, *11*, 5132.

[20] L. Xie, X. Xiong, Q. Chang, X. Chen, C. Wei, X. Li, M. Zhang, W. Su, Z. Cui, *Small*, **2019**, *15*, 1900111.

[21] M. D. Ho, D. Kim, N. Kim, S. M. Cho, H. Chae, *ACS Appl. Mater. Interfaces*, **2013**, *5*, 12369.

[22] L. Bai, X. Yang, C. Y. Ang, K. T. Nguyen, T. Ding, P. Bose, Q. Gao, A. K. Mandal, X. W. Sun, H. V. Demir, Y. Zhao, *Nanoscale*, **2015**, *7*, 11531.

[23] W. Zhao, L. Xie, Y.-Q.-Q. Yi, X. Chen, J. Hu, W. Su, Z. Cui, *Mater. Chem. Front.*, **2020**, *4*, 3368.

[24] S. Lee, S.-O. Kim, H. Shin, H.-J. Yun, K. Yang, S.-K. Kwon, J.-J. Kim, Y.-H. Kim, *J. Am. Chem. Soc.*, **2013**, *135*, 14321.

[25] S. O. Jeon, S. E. Jang, H. S. Son, J. Y. Lee, *Adv. Mater.*, **2011**, *23*, 1436.

[26] J.-L. Brédas, D. Beljonne, V. Coropceanu, J. Cornil, *Chem. Rev.*, **2004**, *104*, 4971.

[27] M. Redecker, D. D. C. Bradley, M. Inbasekaran, W. W. Wu, E. P. Woo, *Adv. Mater.*, **1999**, *11*, 241.

[28] X. Yang, G. Zhou, W.-Y. Wong, *Chem. Soc. Rev.*, **2015**, *44*, 8484.

[29] Z. Yang, Q. Wu, G. Lin, X. Zhou, W. Wu, X. Yang, J. Zhang, W. Li, *Mater. Horiz.*, **2019**, *6*, 2009.

[30] W. Cao, C. Xiang, Y. Yang, Q. Chen, L. Chen, X. Yan, L. Qian, *Nat. Commun.*, **2018**, *9*, 2608.

[31] X. Li, Q. Lin, J. Song, H. Shen, H. Zhang, L. S. Li, X. Li, Z. Du, *Adv. Optical Mater.*, **2020**, *8*, 1901145.

[32] C. Xiang, L. Wu, Z. Lu, M. Li, Y. Wen, Y. Yang, W. Liu, T. Zhang, W. Cao, S.-W. Tsang, B. Shan, X. Yan, L. Qian, *Nat. Commun.*, **2020**, *11*, 1646.

[33] D. Liu, S. Cao, S. Wang, H. Wang, W. Dai, B. Zou, J. Zhao, Y. Wang, *J. Phys. Chem. Lett.*, **2020**, *11*, 3111.

[34] Z. Chen, H. Zhang, D. Wen, W. Wu, Q. Zeng, S. Chen, W.-Y. Wong, *Chem. Sci.*, **2020**, *11*, 2342.

[35] H. Usta, D. Alimli, R. Ozdemir, S. Dabak, Y. Zorlu, F. Alkan, E. Tekin, A. Can, *ACS Appl. Mater. Interfaces*, **2019**, *11*, 44474.

[36] J. Hwang, C. Lee, J.-E. Jeong, C. Y. Kim, H. Y. Woo, S. Park, M. J. Cho, D. H. Choi, *ACS Appl. Mater. Interfaces*, **2020**, *12*, 8485.

[37] J. He, Z. Huang, Z. Huang, S. Liao, F. Peng, Z. Zhong, T. Guo, L. Ying, Y. Cao, *J. Mater. Chem. C*, **2019**, *7*, 13859.

[38] G. Qian, Z. Zhong, M. Luo, D. Yu, Z. Zhang, D. Ma, Z. Y. Wang, *J. Phys. Chem. C*, **2009**, *113*, 1589.

[39] Z. Chen, C.-L. Ho, L. Wang, W-.Y. Wong, *Adv. Mater.*, **2020**, *32*, 1903269.

[40] S. A. Jenekhe, J. A. Osaheni, *Science*, **1994**, *265*, 765.

[41] Y. Baek, Y. Kwon, C. Maeng, J. H. Lee, H. Hwang, K. M. Lee, P. H. Lee, *J. Org. Chem.*, **2019**, *84*, 3843.

[42] J. Jiang, Z. Xu, J. Zhou, M. Hanif, Q. Jiang, D. Hu, R. Zhao, C. Wang, L. Liu, D. Ma, Y. Ma, Y. Cao, *Chem. Mater.*, **2019**, *17*, 6499.

[43] T. Sudyoadsuk, P. Chasing, T. Kaewpuang, T. Manyum, C. Chaiwai, S. Namuangruk, V. Promarak, *J. Mater. Chem. C*, **2020**, *8*, 5045.

[44] X. Zhao, Z.-K. Tan, *Nat. Photonics*, **2020**, *14*, 215.

[45] Z. Chen, L. Wang, C.-L. Ho, S. Chen, S. Suramitr, A. Plucksacholatarn, N. Zhu, S. Hannongbua, W.-Y. Wong, *Adv. Optical Mater.*, **2018**, *6*, 1800824.

[46] K.-H. Lee, C.-Y. Han, H.-D. Kang, H. Ko, C. Lee, J. Lee, N. Myoung, S.-Y. Yim, H. Yang, *ACS Nano*, **2015**, *9*, 10941.

[47] P. Shen, X. Li, F. Cao, X. Ding, X. Yang, *J. Mater. Chem. C*, **2018**, *6*, 9642.

[48] W. K. Bae, J. Lim, D. Lee, M. Park, H. Lee, J. Kwak, K. Char, C. Lee, S. Lee, *Adv. Mater.*, **2014**, *26*, 6387.

[49] H. Zhang, Q. Su, Y. Sun, S. Chen, *Adv. Optical Mater.*, **2018**, *6*, 1800354.

[50] Y. Zhu, R. Xu, Y. Zhou, Z. Xu, Y. Liu, F. Tian, X. Zheng, F. Ma, R. Alsharafi, H. Hu, T. Guo, T. W. Kim, F. Li, *Adv. Optical Mater.*, **2020**, *8*, 2001479.

[51] H.-W. Mo, Y. Tsuchiya, Y. Geng, T. Sagawa, C. Kikuchi, H. Nakanotani, F. Ito, C. Adachi, *Adv. Funct. Mater.*, **2016**, *26*, 6703.

A new polymer CNPr-TFB with high hole conductivity and stabilized HOMO was used as a hole transporting polymer for QLED applications. It affords RGB and white QLEDs with the peak EQEs of 20.7%, 16.6%, 11.3% and 15.0%, respectively, which are superior to those of TFB based devices. Therefore, CNPr-TFB could be an excellent hole transporting polymer for further QLED applications.

Keyword hole transporting polymers, stabilized HOMOs, high hole conductivities, high efficiencies, quantum dot light-emitting diodes

W. Wu, Z. Chen,* Y. Zhan,* B. Liu, W. Song, Y. Guo, J. Yan, X. Yang, Z. Zhou and W.-Y. Wong*

An efficient hole transporting polymer for quantum dot light-emitting diodes